GaN Nanowires Grown by Molecular Beam Epitaxy

Kris A. Bertness, *Senior Member, IEEE*, Norman A. Sanford, and Albert V. Davydov

(Invited Paper)

***Abstract*—The unique properties of GaN nanowires grown by molecular beam epitaxy are reviewed. These properties include the absence of residual strain, exclusion of most extended defects, long photoluminescence lifetime, low surface recombination velocity, and high mechanical quality factor. The high purity of the nanowires grown by this method allows for controllable n-type doping. P-type doping presents more challenges but has been demonstrated in active light-emitting diode devices. The present understanding of nucleation and growth of these materials is also reviewed.**

***Index Terms*—Crystal growth, nanotechnology, photoluminescence, semiconductor materials.**

I. Introduction

SEMICONDUCTOR nanostructures have opened many new paths for device technology and fundamental studies. This is particularly true for (Al, In, Ga)N nanowires because of the difficulty in growing large single crystals in this alloy family to serve as substrates for epitaxial growth. Nanowire growth is, therefore, one of the few methods available to produce low-strain, defect-free material.

This review describes the unique properties of GaN nanowires and their related alloys when grown by catalyst-free molecular beam epitaxy (MBE). Many of their properties stem directly from the growth method. Unlike catalyst-based methods commonly used to grow nanowires, MBE growth of GaN nanowires is driven by differences in surface energies, sticking coefficients, and diffusion coefficients on different crystal planes. The growth proceeds at high temperature and with low growth rate, allowing the crystals to fully relax and achieve a structure that annihilates crystalline defects. The high purity of the starting materials and ultrahigh vacuum environment prevents incorporation of chemical impurities.

The earliest reports of GaN nanowire growth by this method appeared from Sophia University, Tokyo [1], [2] and the Universidad Politécnica, Madrid [3], [4]. Since then, morphology and optical property descriptions have been reported by numerous other groups [5]–[9]. Electrical characterization and device results are more infrequent, but they include single nanowire field effect transistors (FETs) [10] and light-emitting diodes (LEDs) made of ensembles of nanowires [11]. More recent study will be discussed in the main sections of this paper, along with the growth mechanism developments over the past several years.

GaN nanowires can also be grown by other mechanisms, though the quality of this material varies widely and in many cases has not been fully explored with sensitive methods such as low-temperature photoluminescence (PL) or carrier lifetime measurements. Although this study in general falls outside the scope of this review, excellent device results have been demonstrated with catalyst-grown GaN nanowires by use of organometallics vapor-phase epitaxy (OMVPE) for LEDs [12] and FETs [13]. LEDs have also been fabricated from ensembles of GaN nanowires grown by catalyst-free OMVPE with patterned substrates [14] and by hydride vapor-phase epitaxy (HVPE) [15]. Other crystal growth methods that have demonstrated GaN nanowire morphology include metalorganic MBE [16], OMVPE with anodic alumina templates [17], direct reaction [18]–[21], catalyst OMVPE [22], [23], and HVPE [24]–[29]. Because these materials have been defined more by their morphology than by their electrical or optical properties, what we refer to in this study as GaN nanowires have also been variously called GaN nanorods, nanocolumns, and nanowhiskers.

The broader field of nanowire growth includes many other materials and growth methods. The reader is referred to [30] for a review of inorganic nanowire growth, [31] for a high-level review covering many materials mostly grown by catalyst methods, and [32] for a semiconductor nanowire review covering mostly catalyst and direct growth. An overview of catalyst-based OMVPE nanowire growth is provided in [33].

II. Growth

A. Growth Parameters and Morphology

GaN nanowires grown by catalyst-free MBE form exclusively in the wurtzite (or hexagonal) crystal structure [34] with the growth axis parallel to the [0 0 0 1] crystal direction, also called the c-axis. The sidewalls of the nanowires conform to the $\{1\,0\,0\}$ family of m-planes. When the nanowires are well separated, their cross sections will be near perfect hexagons, as shown in the field-emission scanning electron microscopy (FESEM) images in Fig. 1(b). The nanowires generally have Ga-face polarity, i.e., the Ga–N bonds parallel to the growth axis are oriented such that Ga is nearest to the root of the bond and N is nearest to the tip [35], [36], although one study found mixed polarity [37].The Ga-face polarity in GaN films has generally been identified as the smoother surface, but there has been some controversy

Manuscript received July 8, 2010, revised September 2, 2010; accepted September 3, 2010. Date of publication December 6, 2010; date of current version August 5, 2011.

K. A. Bertness and N. A. Sanford are with the National Institute of Standards and Technology, Boulder, CO 80305 USA (e-mail: bertness@boulder.nist.gov; sanford@boulder.nist.gov).

A. V. Davydov is with the National Institute of Standards and Technology, Gaithersburg, MD 20899 USA (e-mail: davydov@nist.gov).

Color versions of one or more of the figures in this paper are available online at http://ieeexplore.ieee.org.

Digital Object Identifier 10.1109/JSTQE.2010.2082504

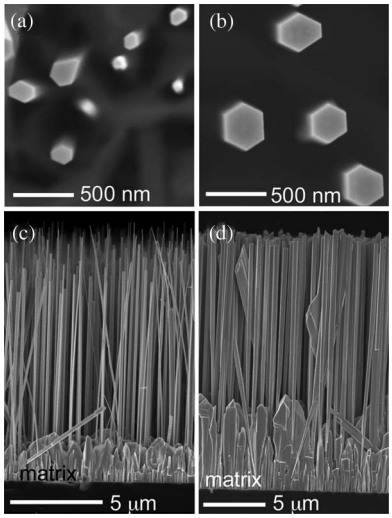

Fig. 1 Examples of GaN nanowire morphology for well-separated nanowires. (a) and (c) Top and side views of the same growth run (66 h growth). (b) and (d) From a different run with higher Ga flux (72 h growth).

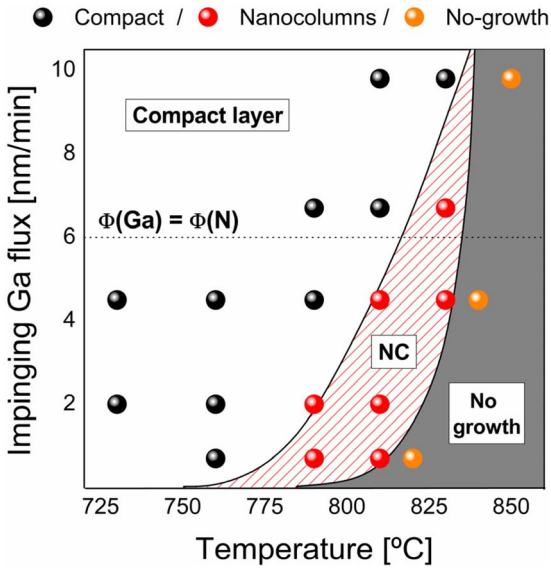

Fig. 2. Phase diagram for GaN nanowire formation at fixed N_2 plasma conditions. Reprinted with permission from [46]. Copyright 2009, American Institute of Physics.

in measurements on bulk crystals [38]. Si(1 1 1) is the most commonly used substrate, and the nanowires will predominantly align azimuthally to the underlying Si such that the GaN$\langle 1\,1\,\bar{2}\,0\rangle$ directions are parallel with the Si$\langle 1\,\bar{1}\,0\rangle$ directions [8], [39]. Thin AlN buffer layers are commonly used to prevent reactions between Ga and Si and to increase the uniformity of the nanowire nucleation process [35], [40]. GaN nanowires have also been grown on sapphire [1], [41] and Si(1 0 0) substrates. Growth on Si(1 0 0) leads to less regular morphology [40], [42] but has been shown to have PL similar to material grown on Si(1 1 1) [43], [44].

GaN nanowires typically form under MBE growth conditions of high active N flux relative to Ga flux and high substrate growth temperature, 740–830 °C being typical of the ranges reported. Group III elements (Ga, Al, In) are supplied by direct evaporation from molten metal in standard Knudsen cells. The N source is a gas injector with active excitation of the gas, typically provided by maintaining a plasma with radio-frequency (RF) excitation. This plasma-assisted or RF-assisted N_2 stream consists of a mixture of atomic N and excited molecular states that react readily with Ga at the growth surface. The beam can also contain ionized species, although many sources include biased plates designed to deflect any charged species from reaching the substrate. The relative abundances of these species vary with RF power, gas flow rate, plasma pressure, and details of the plasma tube and confinement fields. Optical emission from the plasma is frequently used as a semiquantitative measure of the relative abundance of these species [45], but aperture design and bias plates also influence the composition of the N flux that actually reaches the growing material. The variability in N_2 source operation coupled with the difficulty in monitoring the species produced is a major factor in the variability of results from different growth systems and long-time-period drift within a single system.

As described succinctly in [46], the morphology transitions from compact films to nanowires to the absence of growth from complete reevaporation of Ga. The transition temperatures depend on the Ga flux and N flux, as shown in the phase diagram given in Fig. 2. Within the nanowire (nanocolumn) growth regime, the density and diameter of nanowires can be influenced by changes in the Ga flux, substrate temperature and N_2 plasma conditions. Nanowire density is strongly affected by buffer layers and initial growth conditions. The amount of material that grows between the nanowires, which we call the matrix layer, also varies, from a relatively thick, faceted layer, such as that illustrated in Fig. 1, to a dense layer with no apparent matrix but irregular nanowire shapes [47] to very sparse nanowires with no matrix [39]. The matrix layer is often quasi-columnar, making the distinction between it and the nanowires difficult to identify in some cases. Additional examples of MBE GaN nanowire morphologies can be found in [48] and [49].

The Ga flux and substrate temperature also present some measurement challenges. Although most MBE systems are equipped with a beam flux monitor, the sensitivity of these gauges varies over time due to accumulation of deposits on active components. Changes in sensitivity by a factor of 2 have been reported [42]. More accurate results can be obtained by measuring the Ga flux under identical cell conditions but with the substrate held at lower temperatures where the Ga sticking coefficient can be assumed to be 1. The Ga flux can be calculated from *in situ* optical reflectance measurements [4], *ex situ* layer thickness measurements [50], or GaAs reflection high-energy electron diffraction (RHEED) intensity oscillations (if the MBE system has GaAs growth capability) [40]. The measurement of substrate temperature in MBE systems has a long history. The most accurate measurements at these high temperatures are typically achieved with optical pyrometry. The sample emissivity must be known for accurate calibration [51], and changes in emissivity during growth can lead to a systematic drift in the calibration. Using a calibrated pyrometer that collects light from the backside of the

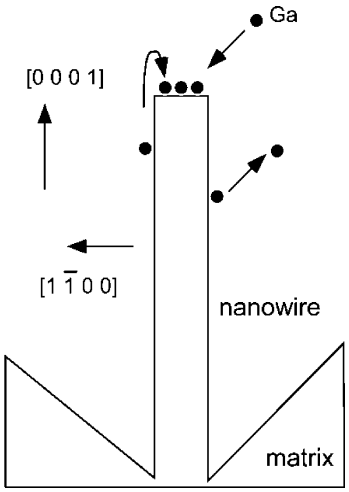

Fig. 3. Schematic of growth propagation mechanism for GaN nanowires grown by MBE. The vertical growth is driven largely by the much lower sticking coefficient for Ga on the sidewall m-planes relative to the top surface c-planes.

substrate, where no deposition occurs, we have been able to estimate that substrate temperature can be inaccurate by as much as 15 °C when uncorrected for changes in surface emissivity.

B. Nucleation and Growth Mechanisms

Because of the prevalence of catalyst-based nanowire growth, early workers in the field of GaN nanowire growth by MBE hypothesized that the growth proceeded through the formation of nanoscale Ga droplets acting as self-catalysis particles [49], [52]. A large body of evidence has accumulated in favor of other explanations, however, particularly because Ga droplets were never observed on nanowire tips. The high growth temperatures used for nanowires relative to MBE thin-film growth, the loss of Ga to re-evaporation, slow growth rate, sensitivity to surfactant effects, and consistent crystallography indicated that surface diffusion and variations in sticking coefficients were the primary drivers for growth [53]. This study led to the demonstration of a differential sticking coefficient model [40], [42], [54] of growth propagation, as illustrated in Fig. 3.

Further support for this model comes from recent theoretical predictions of surface energies and diffusion coefficients [55] and tests of growth under unusual conditions, including rapid cooling while continuing growth [42] and intentional Ga droplet formation [48]. As presented so far, this model has not been quantitatively applied to predict growth rates. A complete model would account for the fact that the three-dimensional geometry itself alters the predicted growth rates because the average Ga flux on the top surface is five to six times higher than that on the sidewalls [37], even in the absence of surface diffusion or sticking coefficient variations. There is evidence in [47] and [56] for a significant contribution to nanowire growth from Ga atoms that arrive either at the substrate surface or at the nanowire sidewalls and diffuse to the top surface. These mechanisms predict that thinner nanowires should grow longer than thicker ones. Experimental observations vary on whether this length variation indeed occurs, indicating that there is sufficient variation in growth conditions to argue for aspects of all these models. The length variation is most evident in growth where AlN buffers are omitted, growth periods are short, and there is a significant fraction of nanowires with diameters less than 50 nm.

Nucleation of nanowire growth is typically random, producing a wide range of densities and diameters within a single growth run. This variation increases for comparisons made among different growth systems. Nanowires have been found to nucleate on bare Si with a minimum nucleation diameter of 7 nm [57] to 15 nm [47] and no matrix layer growth. In [35], it was found that nanowires nucleated on AlN buffer layers arose from the top of GaN islands with a density that increased with increasing substrate temperature in the range of 740–800 °C while the nanowire growth rate declined. In another study [48] on nanowire growth on AlN buffer layers, increasing substrate temperature led to larger nanowire nuclei and thereby reduced the nanowire density. Several authors point out that despite the high N_2 flux used for GaN nanowire growth, the N_2 species can limit the vertical growth rates [4], [35], [58]. The N_2 plasma conditions can also affect nanowire nucleation independent of the nanowire growth rate [40]. This study also found that nanowires tended to nucleate inside faceted pits, rather than on the top of islands. A more recent study [59] of the initial GaN nanowire growth on 5-nm AlN layers found several stages of island formation and strain relaxation. High-resolution TEM of nanowire roots frequently shows thin layers of amorphous material, possibly SiN_x, between the substrate and the crystalline region of the nanowire [36], [48], [57]. The variety of possible seed crystal shapes may in part explain why so much variation is observed over relatively small ranges in growth parameter space.

C. Selective Epitaxy

The difficulty in controlling nanowire nucleation has led many workers to explore more complex nucleation schemes. In [11], a method of intentional generation of GaN seed crystals at low growth temperature prior to nanowire growth is described. Patterned epitaxy, in which substrates are masked with patterned layers that limit growth to specific areas, is well known in OMVPE growth and has been used for GaN nanowire growth in OMVPE [60], [61]. Because elemental Ga is more reactive with most mask surfaces, it has taken longer to develop selective epitaxy processes for MBE. Initial attempts with SiO_2 masks [4] and Al pedestal regions [62] produced differences in nucleation density but not true selectivity. Better results have been obtained with Ti masks that are intentionally converted to TiN_x *in situ*, and this method has proved critical in obtaining consistent diameters in nanowires for LEDs (see Fig. 4). Without the diameter control afforded by the selective epitaxy strategy, the In incorporation varies from nanowire to nanowire and the emission wavelength shifts. These experiments also suggest that optical emission from the InGaN disks is most intense when the InGaN quantum well grows on tilted facets rather than as a c-plane disk perpendicular to the growth axis. The faceted morphology avoids spontaneous polarization fields that separate electrons and holes spatially within a c-plane quantum well.

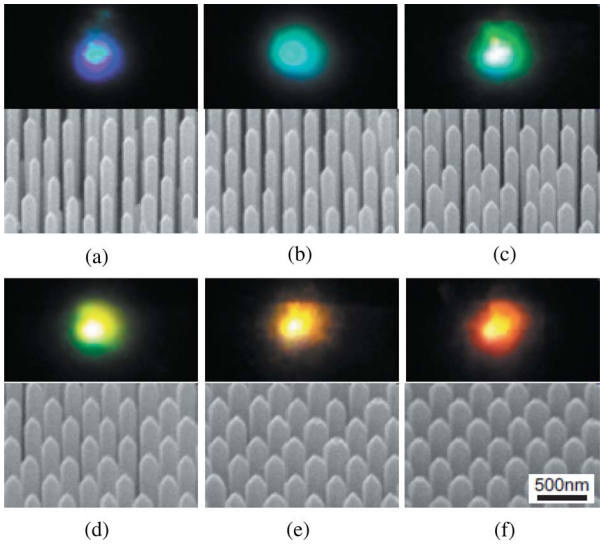

Fig. 4. Bird's eye view SEM and emission images excited by HeCd laser from InGaN/GaN nanowires with diameters as shown. The In incorporation increases with increasing nanowire diameter. Reprinted with permission from [2]. Copyright 2010, American Institute of Physics.

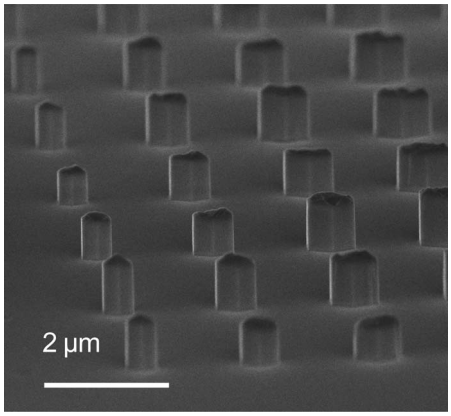

Fig. 5 Selective epitaxial of GaN nanowires through openings in a SiN_x mask covering an AlN buffer layer. The cross sections are equilateral hexagons with diameters that track the size of the mask opening.

The selectivity with TiN_x masks relies on close spacing of the openings to prevent random nucleation on the mask. Near-perfect selectivity, even in large mask regions, has recently been demonstrated with SiN_x masks on AlN buffer layers, as shown in Fig. 5. Details of this result are given in [63].

D. Crystalline Perfection

GaN nanowires grown by MBE are typically free of strain because strain mismatch between the substrate and the growing GaN can readily be relieved by dislocation formation perpendicular to the (0 0 0 1) planes. The small diameter of the wire and ease of dislocation glide within the c-plane allow annihilation of the dislocations at the nanowire surface, leaving the crystal to grow defect-free after a few nanometers of axial growth [64]. Recent studies [59] using RHEED have identified several morphological steps in the nucleation of the nanowires and confirm the confinement of strain relaxation to dislocation formation

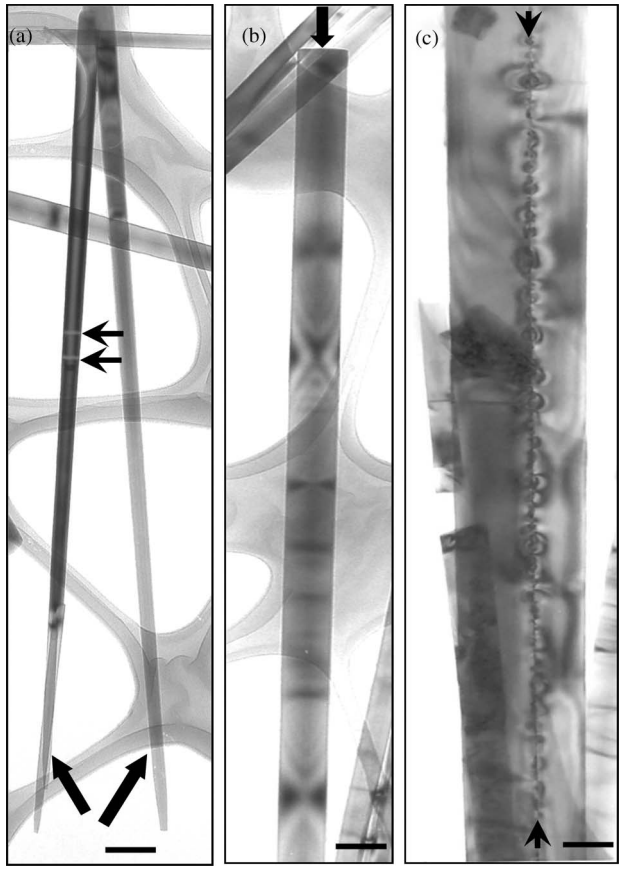

Fig. 6. Bright-field TEM images of GaN nanowires. (a) Bottom portions of two nanowires near their roots (indicated by block arrows); note occasional basal plane stacking faults (horizontal arrows). (b) Defect-free portion of a nanowire near its tip (indicated by block arrow); note band-like contrast associated with nanowire bending. (c) Middle portion of two coalesced nanowires; note a continuous array of dislocations at the NWs interface (indicated by vertical arrows). Scale bar is 100 nm. All images were recorded near the [1 1 0] GaN zone axis orientation. [86]

and annihilation very close to the nanowire-substrate boundary. The perfection of the crystalline structure may be lost if the nanowires coalesce during growth [65], [66]. Fig. 6(a) and (b) shows TEM images of nearly defect-free nanowires and a chain of nanowire defects formed as a consequence of coalescence of two nanowires. Screw dislocations have been observed in GaN nanowires grown on sapphire [67]. Although this observation is not common, elastic theory predicts that screw dislocations are in fact stable if formed near the center of a thin rod [68]. It is problematic to rely on TEM alone for defect identification because of the small number of samples that can be conveniently tested, and the need to examine different diffraction conditions and sample tilts to distinguish defects from bending contrast. Optical measurements, described in the next section, also provide evidence for the high crystalline quality of these materials.

By comparison, the structural properties of a-axis catalyst-grown GaN nanowires are very different [69]. These nanowires are oriented such that dislocations tend to propagate along the nanowire length. Basal plane (c-plane) stacking faults are also common, leading to regions of the crystal with a structure that more closely resembles that of cubic GaN. The high speed

of catalyst-based growth and the lower purity environments in which such growth often takes place can lead to high defect incorporation both from crystallographic imperfections and chemical impurities [70], [71]. These effects can be mitigated to some degree by employing the lowest possible growth rates and using high-purity environments such as MBE and OMVPE. A recent comparison [72] of catalyst versus catalyst-free MBE nanowires found that even under the same growth conditions, catalytic growth produced material with a high density of basal plane stacking faults, as determined by TEM. The PL intensity was also lower for catalyst-grown material, but the spectrum was free of yellow luminescence. OMVPE materials consistently contain a higher impurity background, presumed to be carbon, especially apparent in material grown at lower substrate temperatures. It is not clear, however, if carbon incorporation is necessarily detrimental to device operation provided that the concentration is below the point where significant subgap luminescence is observed [73].

E. Heterojunctions and Alloys

Nanowires of purely binary InN [74]–[76], AlN [77], and alloys of these compounds with GaN have been grown by MBE and other methods. As illustrated in the previous section, the addition of InGaN quantum disks in GaN nanowires [11], [78] is particularly useful for optoelectronic devices to enhance luminescence and tune the wavelength of the emission. Compelling results have also been obtained for GaN disks in AlGaN wires [79]. In [4], a comprehensive overview of these types of heterostructures is given, and we mention here just some highlights of this study. The interfaces between the AlGaN and GaN are atomically abrupt, and the quantization of the energy states in the quantum disks has been established [80]. Bragg reflector stacks of alternating AlN and GaN layers were also grown, demonstrating the ability of the nanowire structure to withstand strain without cracking [79]. One important outcome of this investigation was the determination that variations in strain between the core of the nanowire and its outer surface could lead to changes in the band structure that suppress radiative recombination of electrons and holes by spatially separating the two carrier types [81].

In Fig. 7, we illustrate another type of heterostructure, a core-sleeve *p-n* junction. This structure was fabricated by coating n-type MBE-grown nanowires with p-type layers grown with HVPE. The image contrast depends on electron beam energy and likely arises from differences in work function between the p-type and n-type regions. The exact correlation between the physical junction and the boundary imaged by FESEM has not been established.

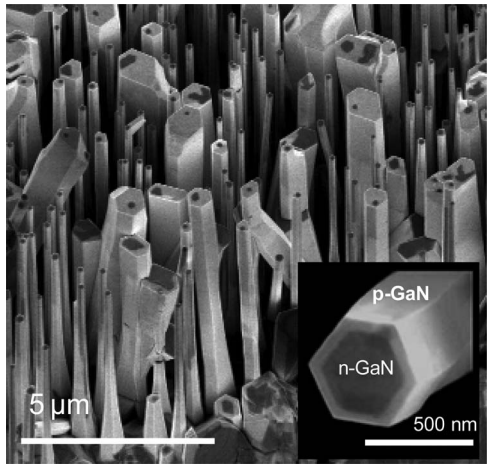

Fig. 7. FESEM images of core-sleeve *p-n* junctions formed by overgrowth of p-type HVPE GaN on MBE-grown GaN nanowires [87].

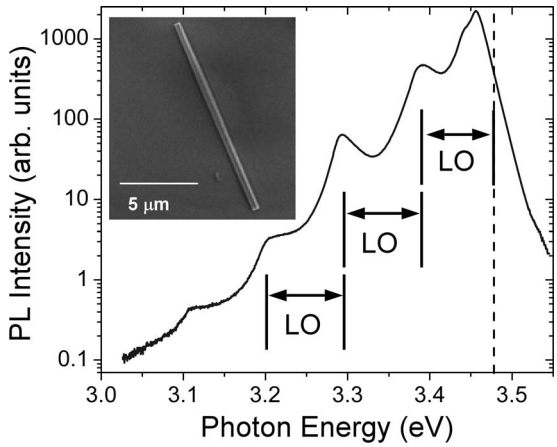

Fig. 8. Low-temperature photoluminescence of a single GaN nanowire showing that the spectrum consists of only exciton transitions and phonon replica peaks of free exciton transitions. The donor-bound exciton emission is shifted from the unstrained position, marked with the dashed line at 3.472 eV, by strain applied to the nanowire by differential thermal contraction of the nanowire relative to its substrate [88].

III. Optical Properties

A. Photoluminescence (PL)

Investigation of the optical properties of MBE-grown GaN nanowires provided some of the earliest evidence for their exceptional quality. Room-temperature PL intensity from these nanowires usually compares favorably with that from reference GaN films [53], [82], though the variety of quality among GaN materials prevents definitive comparisons. The low-temperature PL spectrum generally consists solely of donor-bound excitons, free excitons, and the associated phonon-mediated replicas of these transitions (see Fig. 8). In nanowires with radii below 40 nm, a two-electron satellite peak has also been reported [44] and its enhanced intensity attributed to interactions between the exciton pairs and nearby surfaces. For isolated nanowires, the donor-bound exciton D^0X_A peak is found at the strain-free position of 3.472 eV [83]–[85]. These data, in addition to X-ray diffraction on nanowire ensembles [8], [53], demonstrated that the growth mode of the nanowires promoted complete relaxation of lattice mismatch early in the nucleation stage without propagation of dislocations along the nanowire axis.

The absence of strain broadening allowed exceptionally high-resolution spectroscopy relative to that obtainable from GaN specimens grown by other methods, so polarization anisotropy of the exciton peaks could be monitored from 3.2 to 300 K [83].

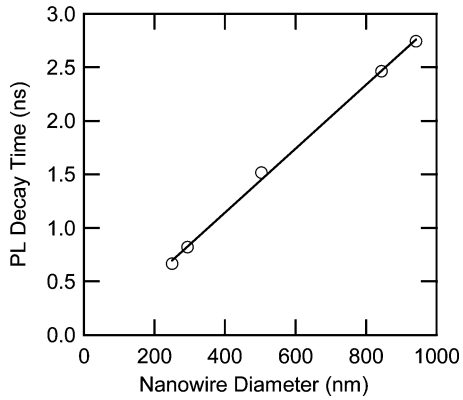

Fig. 9. Linear fit of PL decay time vs. nanowire diameter extracts the surface recombination velocity for this set of nanowires (from the same growth run).

Low-temperature PL peaks as narrow as 300 μeV have been reported [89]. Yellow luminescence is generally absent from well-formed nanowires but is occasionally reported for larger, coalesced structures [65], material grown at lower temperatures [49], and specimens that contain matrix layer material [66]. Subgap luminescence in GaN (including yellow luminescence) is indicative of chemical impurities and/or structural defects [90].

The inherently strain-free state of the growth mode of the nanowires in turn permits the monitoring of strain states by monitoring shifts in the PL spectrum. The data in Fig. 8 show how the D^0X_A peak shifts to lower energy because of tensile strain imposed on the nanowire by its adhesion (via van der Waals bonding) to a quartz substrate during cooling to $\sim$5 K. Compressive strain from atomic layer deposition of alumina produced positive shifts [88].

Time-resolved PL data indicate that the dominant recombination processes vary considerably with temperature. The low-temperature regime is dominated by radiative recombination of bound excitons, and the thermalization of these exciton pairs away from the shallow donor that binds them causes the PL lifetime to decrease initially as the temperature increases [88]. The lifetime begins to increase in the range near 150 K as free exciton recombination becomes dominant, provided that nonradiative recombination processes are saturated. Near room temperature, surface recombination becomes the limit to the PL lifetime, so that thicker nanowires have longer lifetimes (see Fig. 9). Although this limit certainly invites attempts at surface passivation with AlGaN layers and other schemes applied in GaN epitaxial layers, we note that the actual value of the surface recombination velocity, 9×10^3 cm$\cdot$s^{-1}, is quite low compared with that of other compound semiconductor surfaces, e.g., GaAs [91].

This variation in recombination mechanisms over different temperature regimes underscores the need to make careful measurements of lifetime to estimate internal quantum efficiency (IQE). Ratios of room-temperature PL intensity to low-temperature PL intensity do not compare the same phenomena and, therefore, do not reveal the room-temperature IQE. It cannot be assumed that the IQE is 100% at low temperature, nor is the "bulk" lifetime of the nanowire material likely to control recombination at room temperature. These caveats apply to epitaxial InGaN/GaN films as well [92]. By varying excitation conditions and sample temperature T until a characteristic $T^{3/2}$ dependence is observed in the PL lifetime, we have estimated that the IQE of one of our moderately doped GaN nanowires is 30% at room temperature [93]. This value is for excitation with 266-nm light in 8-ns pulses of 190 FJ/cm^2, with a 15 kHz repetition rate. The lifetime is limited by surface recombination, but the exact nature of the surface states is undetermined.

B. Cathodoluminescence

Several groups have examined GaN nanowires grown by MBE with cathodoluminescence (CL). This method offers more localized excitation and ready correlation between luminescence and structure [49] [85], [94]. The rapid diffusion of carriers from the absorption site, however, limits the lateral resolution of the method to within a factor of 2 or 3 of what can be achieved with PL. CL has been used to show that subgap luminescence (yellow or blue) is correlated with coalesced regions or other anomalous growth structures [65], [66]. Dispersed GaN nanowires readily acquire static charge in vacuum, causing a reversible decrease in CL intensity [66]. Electron-beam-induced deposits or damage must be considered in interpretation of the data. One interesting application of CL has been to map minority carrier diffusion length in OMVPE-grown GaN nanowires [95] by collecting luminescence with imaging systems or near-field scanning optical microscopy.

IV. Electrical Properties

A. Carrier Concentration and Mobility

Because ultrahigh-vacuum MBE technology and high growth temperature are employed in their fabrication, GaN nanowires have very low concentrations of chemical impurities. Their added exclusion of crystalline defects leads to very low background carrier concentrations, on the order of 10^{15} cm^{-3} or less. A wide range of n-type doping concentrations can readily be achieved with Si as an intentional dopant. The nanowire morphology, however, presents significant challenges in unequivocal determination of carrier type and measurement of free carrier concentration N, and drift mobility μ. P-type doping with Mg has been reported by several groups who have fabricated ensemble LEDs, but the absence of ohmic behavior for single p-type nanowires continues to impede true electrical characterization of their properties. This section will therefore be restricted to discussion of n-type nanowires.

Numerous articles have appeared illustrating the use of nanowire FET devices as test structures to infer these quantities [28], [96], [97]. Typical sample geometry consists of a nanowire dispersed onto an oxidized Si substrate with source and drain contacts fabricated at the two nanowire ends. The Si substrate itself is biased to form a "back gate," and the capacitance between the nanowire and the substrate is modeled as an ideal conducting wire embedded in a dielectric material far above a conducting plane. There are a number of systematic errors introduced by this approach [98], [99]. The full three-dimensional

TABLE I
PARAMETER RANGES FOR RESISTANCE ANALYSIS OF GaN NANOWIRE BATCHES FROM DIFFERENT GROWTH RUNS

Φ[eV]	N [cm^{-3}]	μ [cm^2·V^{-1}·s^{-1}]
Batch 1: intentional Si doping		
0.5 – 0.6	6—10 x 10^{17}	600—300
0.4	5—8 x 10^{17}	800—500
Batch 2: undoped with high background		
0.5 – 0.6	9—18 x 10^{16}	300—100
0.2 – 0.3	4—8 x 10^{16}	700—200

morphology cannot be ignored in efforts to reliably fit FET simulations to actual device behavior. These systematic errors can also depend on the nanowire diameter, and thus can confer diameter dependence to the mobility determination where none actually exists. Moreover, little is known regarding charge-trapping effects in gate oxide layers, or nanowire-metal interfaces in Schottky-gated nanowire MESFET devices. Fitted FET parameters (transconductance, threshold, and pinchoff) can thus vary widely. A few examples of nanowire FET gate hysteresis and memory effects have been published [10], [97]. Until better models are developed and processing-induced surface and interface artifacts can be eliminated or accounted for, nanowire transport properties inferred from FET behavior should be viewed with caution.

In efforts to infer transport properties from simpler two-terminal nanowire test structures, we have analyzed steady-state dark conductivity and photoconductivity (PC) in collections of these devices fabricated from common growth runs where the nanowires were chosen to have a distribution of diameters [100], [101]. We have found that modeling resistance as a function of nanowire length, radius, and contact area for sets of ten or more n-type (Si-doped) GaN nanowires from the same growth run gives carrier concentration and mobility results with moderate uncertainty. Key assumptions in this analysis are that the dopant concentration and surface potential are uniform across the sample set, the contact resistivity is known, and the surface potential can be assumed to fall within a range of a few electron volts.

These conductivity data allow us to restrict the space of allowable N and μ given a particular range of upward bending Φ of the conduction band at the nanowire surface. The latter controls the thickness of the surface depletion layer. Numerical results for two GaN nanowire growth runs are given in Table I. Disagreement exists in the literature concerning the proper range of Φ for air-exposed GaN. Hall mobility and XPS studies on (air-exposed) MBE GaN films favor the higher μ and lower Φ ranges in Table I. For example, μ in the range 500–700 cm^2·V^{-1}·s^{-1} for GaN with $N \sim$ mid-10^{16} cm^3 is consistent with the results in [102]. $\Phi \sim$ 0.5–0.3 eV is consistent with reports of XPS of clean and air-exposed GaN (0 0 0 1) surfaces [103]. However, Kelvin probe studies of air-exposed c-plane [104], [105] and a-plane [106] GaN surfaces consistently give $\Phi \sim 1$ eV and higher, so the matter is still open to debate.

We have discussed "fast" ($\sim$ns) surface recombination phenomena within the context of time-resolved PL. We also observe

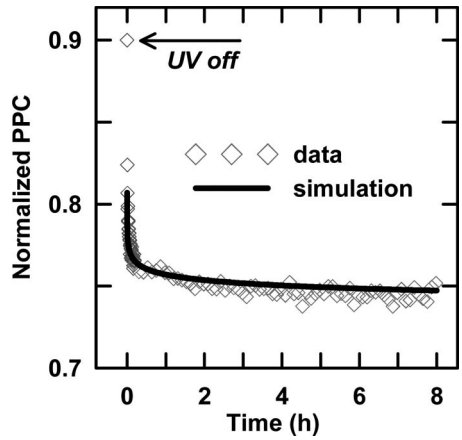

Fig. 10. Fit of phenomenological PPC decay model to data is shown. The UV excitation is blocked at the point indicated, and the PPC decays in the dark. The fit recovers a free carrier concentration of $N = 4 \times 10^{17}$ cm^{-3} and capture cross section $\sigma = 8 \times 10^{-21}$ cm^2 for electrons, as explained in the text.

"slow" changes (over periods of seconds to hours) in surface band bending as revealed in the decay of persistent photoconductivity (PPC) transients. We presented a model describing this effect [101] that was based on a prior phenomenological theory of surface photovoltage on GaN films [104]. In these experiments, the current through a nanowire was monitored while UV light is turned on and off. The photoexcited holes were swept to the surface of the nanowire, reducing the surface band bending and depletion layer thickness. This change increased the diameter of the neutral region within the nanowire and hence the nanowire conductivity. When illumination ceased, equilibrium was restored via free electrons in the bulk of the nanowire surmounting the surface barrier and recombining with trapped holes. These recombination dynamics may be derived from an approximate Shockley–Read–Hall (SRH) analysis that assumes Fermi level pinning near midgap at the surface [107].

An example of fitting this SRH theory to PPC decay for a Batch 1 nanowire is illustrated in Fig. 10. The data are normalized from separate experiments and illustrate that the maximum relative photocurrent rises to 90% of the flatband value under continuous excitation of $\sim$3.6 mW/cm^2 at 360 nm. The fitted PPC simulation is delayed until Φ has recovered sufficiently such that the cylindrical depletion approximation implicit to the model is valid [101]. The fitted solution returns $N = 4 \times 10^{17}$ cm^{-3} and a capture cross section $\sigma = 8 \times 10^{-21}$ cm^2 for electrons by the surface centers. The nanowire diameter between hexagonal vertices is 660 nm. The fitted magnitude of capture cross section is on the low end of the range generally reported for semiconductors (e.g., 10^{-22} to 10^{-12} cm^2) [108]. On the other hand, it is consistent with the long PPC decay times observed and with "slow" surface recombination associated with surface adsorbates and oxide layers [105], [108]. Applying the same fitting procedure to Batch 2 samples discussed above returned N in the mid-10^{16}cm^{-3} range with σ spanning 10^{-23} to 10^{-19} cm^2. These free carrier concentrations are consistent with results from the resistivity study summarized in Table I.

The spectral dependence of the PC is also an indicator of the quality of the MBE-grown nanowires because the subgap

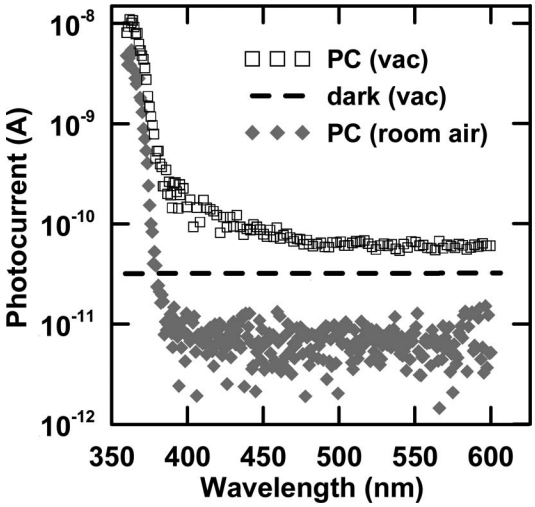

Fig. 11. Weak subgap PC (in ambient room air, and in vacuum) for photoexcitation over the wavelength span indicated. The nanowire sample is chosen such that it is depleted in the dark in ambient air.

photoresponse is weak as compared to that for above-band-gap excitation. However, interpretation of these data should also consider ambient conditions. Fig. 11 illustrates the PC spectral dependence of a nanowire that is depleted in the dark while in room air. For excitation $>$ 380 nm, the PC is at the dark (noise) level, which is roughly three orders of magnitude less than that under band-edge illumination. Under vacuum (mid-10^{-3} Pa), the dark current increases and subgap PC becomes measurable. The excitation intensity over the spectral range indicated is within a factor of 2 of 0.2 mW·cm^{-2}. In contrast to the data in Fig. 11, PC studies on catalyst-grown GaN nanowires have identified specific subgap features [109].

B. GaN Nanowire FETs and High-Frequency Measurements

Although FET properties are not readily converted into measurements of carrier concentration and mobility, the performance of GaN nanowire FETs is promising for applications that require high sensitivity and on–off ratio. GaN FETs made with Schottky barrier gates exhibit subthreshold voltage swings approaching 60 mV/decade and on–off ratios $> 5 \times 10^8$ [10]. Fig. 12(a) shows an image of one such device, and Fig. 12(b) illustrates the pinchoff condition for increasing drain–source voltages. The low threshold voltage of -3.7 V indicates that this omega-gate architecture takes advantage of the large surface-to-volume ratio available in nanowires.

MBE-grown GaN nanowires fabricated with one ohmic and one Schottky contact have also been adapted for high-frequency measurements [110]. The broadband microwave reflection coefficients from about 1 to 10 GHz have been measured for one such structure, and the results fitted to estimate N. More sophisticated modeling and better understanding of interfacial effects are required to improve accuracy, but the demonstration shows that high-frequency capacitance measurements of N may be feasible.

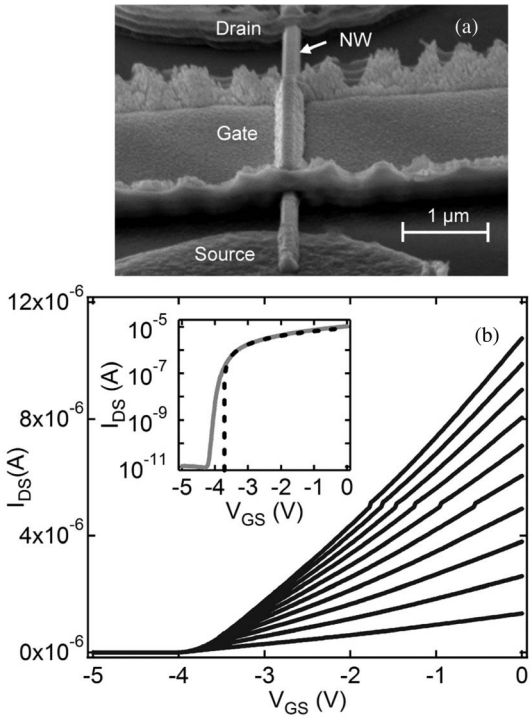

Fig. 12. (a) Device structure and (b) drain–source current ($I_{\rm DS}$) versus gate–source voltage ($V_{\rm GS}$) for a single nanowire MESFET. The bottommost trace corresponds to a drain–source voltage ($V_{\rm DS}$) of 0.1 V, with $\Delta V_{\rm DS} = 0.1$ V between successive traces proceeding upward. Instrument artifacts produced the kink at $I_{\rm DS} = 5$ μA. The inset is a log–linear plot of $I_{\rm DS}$ (solid) and a fit to the above-threshold linear region (dashed) versus $V_{\rm GS}$ for $V_{\rm DS} = 1$ V [10].

V. Mechanical Properties

One of the more interesting properties of MBE-grown GaN nanowires is that they display very high mechanical quality factors, Q, for an object with volume under 1 μm^3. The first evidence for high Q came from SEM observations of spontaneous resonances such as those illustrated in Fig. 13. These resonances can be enhanced with piezoelectric feedback to achieve $Q > 1 \times 10^6$ in vacuum at room temperature [111]. These results compare quite favorably with catalyst-grown GaN nanowires, where $Q < 3000$ is typical [112]. The Q is found to be increasing as temperature increases, and is highly sensitive to absorption of small molecules or carbon deposits, indicating possible application as a mass sensor. Similar studies of nanowires coated with atomic layer deposition have shown that the frequency of oscillation can be tuned up or down depending on the stiffness of the coating. Individual nanowires generally recovered their original Q when the coatings were removed [113]. Measurements of GaN nanowire elastic properties with MEMS fixtures [114] and from modeling of the resonance [111] indicate that Young's modulus is equal to the modulus of bulk GaN within the rather large uncertainty. The high Q appears to be related instead to the smooth sidewalls and low chemical reactivity of GaN, so that these devices are free of damping from oxides that tend to reduce Q in silicon-based resonators.

Piezoresistive readout of GaN nanowire bridge structures has also been demonstrated in devices such as the one shown in Fig. 14. Because of the damping imposed by the metal contacts

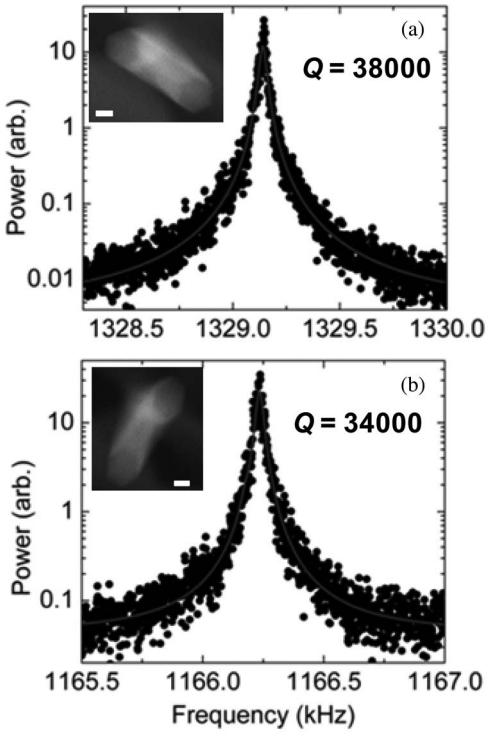

Fig. 13 Two different mechanical resonances of the same GaN nanowire observed with SEM (insets) showing very high-Q under spontaneous excitation. Marker bars in insets are 100 nm; uncertainty in Q values is $\pm$ 2000. Note that (a) one oscillation is along the wide diameter of the nanowire and (b) one is perpendicular to the sidewalls [115].

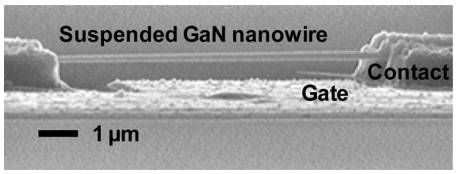

Fig. 14 Bridge structure with GaN nanowire suspended over gate metal to allow capacitive driving of nanowire oscillations and electrical readout of the oscillations [116].

on both ends, $Q \approx$ 1000–2500 is typical for these structures. These devices can operate over a wide range of pressures, though damping by gas molecules also reduces Q.

VI. Conclusion

GaN nanowires grown by MBE currently represent some of the purest specimens of GaN and related alloys. This purity is reflected in their structural, optical, electrical, and mechanical properties. The smooth sidewalls and symmetric growth mode, especially under selective epitaxy processes, offer unique architecture for devices made from this technologically important material. Future study is expected to produce greater variety in heterostructures, parallel fabrication of large ensembles for device applications, and greater ability to measure key optical and electrical properties.

Acknowledgment

The authors would like to thank A. W. Sanders, I. Levin, J. Montague, J. Gray, and C. Rogers for providing unpublished data to make this study more complete.

References

[1] M. Yoshizawa, A. Kikuchi, M. Mori, N. Fujita, and K. Kishino, "Growth of self-organized GaN nanostructures on Al2O3(0 0 0 1) by RF-radical source molecular beam epitaxy," *Jpn. J. Appl. Phys. Part 2*, vol. 36, pp. L459–L462, Apr. 1997.

[2] H. Sekiguchi, K. Kishino, and A. Kikuchi, "Emission color control from blue to red with nanocolumn diameter of InGaN/GaN nanocolumn arrays grown on same substrate," *Appl. Phys. Lett.*, vol. 96, p. 231104, 2010.

[3] M. A. Sánchez-García, E. Calleja, E. Monroy, F. J. Sanchez, F. Calle, E. Munoz, and R. Beresford, "The effect of the III/V ratio and substrate temperature on the morphology and properties of GaN- and AlN-layers grown by molecular beam epitaxy on Si(1 1 1)," *J. Cryst. Growth*, vol. 183, pp. 23–30, Jan. 1998.

[4] E. Calleja, J. Ristic, S. Fernandez-Garrido, L. Ceruffi, M. A. Sanchez-Garcia, J. Grandal, A. Trampert, U. Jahn, G. Sanchez, A. Griol, and B. Sanchez, "Growth, morphology, and structural properties of group-III-nitride nanocolumns and nanodisks," *Physica Status Solidi B—Basic Solid State Phys.*, vol. 244, pp. 2816–2837, Aug. 2007.

[5] Y. S. Park, C. M. Park, D. J. Fu, T. W. Kang, and J. E. Oh, "Photoluminescence studies of GaN nanorods on Si (1 1 1) substrates grown by molecular-beam epitaxy," *Appl. Phys. Lett.*, vol. 85, pp. 5718–5721, 2004.

[6] T. Yamashita, S. Hasegawa, S. Nishida, M. Ishimaru, Y. Hirotsu, and H. Asahi, "Electron field emission from GaN nanorod films grown on Si substrates with native silicon oxides," *Appl. Phys. Lett.*, vol. 86, p. 082109, Feb. 2005.

[7] H. Y. Chen, H. W. Lin, C. H. Shen, and S. Gwo, "Structure and photoluminescence properties of epitaxially oriented GaN nanorods grown on Si(1 1 1) by plasma-assisted molecular-beam epitaxy," *Appl. Phys. Lett.*, vol. 89, p. 243105, Dec. 2006.

[8] K. A. Bertness, J. B. Schlager, N. A. Sanford, A. Roshko, T. E. Harvey, A. V. Davydov, I. Levin, M. D. Vaudin, J. M. Barker, P. T. Blanchard, and L. H. Robins, "High degree of crystalline perfection in spontaneously grown GaN nanowires," in *Proc. GaN, AlN, InN and Related Materials in Materials Science*, Boston, MA, 2005, p. 0892-FF31-03.

[9] R. Calarco, M. Marso, T. Richter, A. I. Aykanat, R. Meijers, A. V. Hart, T. Stoica, and H. Luth, "Size-dependent photoconductivity in MBE-grown GaN-nanowires," *Nano Lett.*, vol. 5, pp. 981–984, May 2005.

[10] P. T. Blanchard, K. A. Bertness, T. E. Harvey, L. M. Mansfield, A. W. Sanders, and N. A. Sanford, "MESFETs Made From Individual GaN Nanowires," *IEEE Trans. Nanotechnol.*, vol. 7, no. 6, pp. 760–765, Nov. 2008.

[11] A. Kikuchi, M. Kawai, M. Tada, and K. Kishino, "InGaN/GaN multiple quantum disk nanocolumn light-emitting diodes grown on (1 1 1)Si substrate," *Jpn. J. Appl. Phys. Part 2*, vol. 43, pp. L1524–L1526, Dec. 2004.

[12] F. Qian, S. Gradecak, Y. Li, C.-Y. Wen, and C. M. Lieber, "Core/Multishell Nanowire Heterostructures as Multicolor, High-Efficiency Light-Emitting Diodes," *Nano Lett.*, vol. 5, pp. 2287–2291, 2005.

[13] S. Vandenbrouck, K. Madjour, D. Theron, Y. J. Dong, Y. Li, C. M. Lieber, and C. Gaquiere, "12 GHz F-MAX GaN/AlN/AlGaN Nanowire MISFET," *IEEE Electron Device Lett.*, vol. 30, no. 4, pp. 322–324, Apr. 2009.

[14] S. D. Hersee, M. Fairchild, A. K. Rishinaramangalam, M. S. Ferdous, L. Zhang, P. M. Varangis, B. S. Swartzentruber, and A. A. Talin, "GaN nanowire light emitting diodes based on templated and scalable nanowire growth process," *Electron. Lett.*, vol. 45, p. 75-U24, Jan. 2009.

[15] H.-M. Kim, Y.-H. Cho, H. Lee, S. I. Kim, S. R. Ryu, D. Y. Kim, T. W. Kang, and K. S. Chung, "High-brightness light emitting diodes using dislocation-free indium gallium nitride/gallium nitride multiquantum-well nanorod arrays," *Nano Lett.*, vol. 4, pp. 1059–1062, 2004.

[16] S.-Y. Kuo, F.-I. Lai, W.-C. Chen, and C.-N. Hsiao, "Catalyst-free growth and characterization of gallium nitride nanorods," *J. Cryst. Growth*, vol. 310, pp. 5129–5133, 2008.

[17] P. Deb, H. Kim, Y. X. Qin, R. Lahiji, M. Oliver, R. Reifenberger, and T. Sands, "GaN nanorod Schottky and p–n junction diodes," *Nano Lett.*, vol. 6, pp. 2893–2898, Dec. 2006.

[18] M. He, P. Zhou, S. N. Mohammad, G. L. Harris, J. B. Halpern, R. Jacobs, W. L. Sarney, and L. Salamanca-Riba, "Growth of GaN nanowires by direct reaction of Ga with NH_3," *J. Cryst. Growth*, vol. 231, pp. 357–365, 2001.

[19] B.-S. Xu, L.-Y. Zhai, J. Liang, S.-F. Ma, H.-S. Jia, and X.-G. Liu, "Synthesis and characterization of high purity GaN nanowires," *J. Cryst. Growth*, vol. 291, pp. 34–39, 2006.

[20] S. Xue, H. Zhuang, C. Xue, L. Hu, B. Li, and S. Zhang, "Growth and characterization of GaN nanorods through ammoniating process by magnetron sputtering on Si(1 1 1) substrates," *Appl. Phys. A-Mater. Sci. Process.*, vol. 87, pp. 645–649, Jun. 2007.

[21] Y. Inoue, T. Hoshino, S. Takeda, K. Ishino, A. Ishida, H. Fujiyasu, H. Kominami, H. Mimura, Y. Nakanishi, and S. Sakakibara, "Strong luminescence from dislocation-free GaN nanopillars," *Appl. Phys. Lett.*, vol. 85, pp. 2340–2342, 2004.

[22] K. Kim, T. Henry, G. Cui, J. Han, Y. K. Song, A. V. Nurmikko, and H. Tang, "Epitaxial growth of aligned GaN nanowires and nanobridges," *Physica Status Solidi B—Basic Solid State Phys.*, vol. 244, pp. 1810–1814, Jun. 2007.

[23] X. J. Weng, R. A. Burke, and J. M. Redwing, "The nature of catalyst particles and growth mechanisms of GaN nanowires grown by Ni-assisted metal-organic chemical vapor deposition," *Nanotechnol.*, vol. 20, p. 085610, Feb. 2009.

[24] Y. S. Won, Y. S. Kim, O. Kryliouk, and T. J. Anderson, "Growth mechanism of catalyst- and template-free group III-nitride nanorods," *J. Cryst. Growth*, vol. 310, pp. 3735–3740, 2008.

[25] K. H. Lee, J. Y. Lee, Y. H. Kwon, S. Y. Ryu, T. W. Kang, H. Y. Jung, S. H. Park, D. U. Lee, and T. W. Kim, "The relation between the microstructural properties and the geometry factors for GaN nanorods formed on Si(1 1 1) substrates," *Solid State Commun.*, vol. 150, pp. 636–639, 2010.

[26] Y. H. Kwon, K. H. Lee, S. Y. Ryu, T. W. Kang, C. H. You, and T. W. Kim, "Formation mechanisms of GaN nanorods grown on Si(1 1 1) substrates," *Appl. Surf. Sci.*, vol. 254, pp. 7014–7017, 2008.

[27] T. Kuykendall, P. Ulrich, S. Aloni, and P. Yang, "Complete composition tunability of InGaN nanowires using a combinatorial approach," *Nature Materials*, vol. 6, pp. 951–956, Dec. 2007.

[28] H. M. Kim, D. S. Kim, D. Y. Kim, T. W. Kang, Y. H. Cho, and K. S. Chung, "Growth and characterization of single-crystal GaN nanorods by hydride vapor phase epitaxy," *Appl. Phys. Lett.*, vol. 81, pp. 2193–2195, Sep. 2002.

[29] G. Seryogin, I. Shalish, W. Moberlychan, and V. Narayanamurti, "Catalytic hydride vapour phase epitaxy growth of GaN nanowires," *Nanotechnol.*, vol. 16, pp. 2342–2345, 2005.

[30] C. N. R. Rao, F. L. Deepak, G. Gundiah, and A. Govindaraj, "Inorganic nanowires," *Progr. Solid State Chem.*, vol. 31, pp. 5–147, 2003.

[31] S. V. N. T. Kuchibhatla, A. S. Karakoti, D. Bera, and S. Seal, "One dimensional nanostructured materials," *Progr. Mater. Sci.*, vol. 52, pp. 699–913, 2007.

[32] S. Barth, F. Hernandez-Ramirez, J. D. Holmes, and A. Romano-Rodriguez, "Synthesis and applications of one-dimensional semiconductors," *Progr. Mater. Sci.*, vol. 55, pp. 563–627, 2010.

[33] W. Seifert, M. Borgström, K. Deppert, K. A. Dicka, J. Johansson, M. W. Larsson, T. Mårtensson, N. Sköld, C. P. T. Svensson, B. A. Wacaser, L. R. Wallenberg, and L. Samuelson, "Growth of one-dimensional nanostructures in MOVPE," *J. Cryst. Growth*, vol. 272, pp. 211–220, 2004.

[34] A. Trampert, O. Brandt, and K. H. Ploog, "Crystal structure of group III nitrides," in *Gallium Nitride (GaN) I*, J. I. Pankove and T. D. Moustakas, Eds. San Diego, CA: Academic, 1998, pp. 167–192.

[35] R. Songmuang, O. Landre, and B. Daudin, "From nucleation to growth of catalyst-free GaN nanowires on thin AlN buffer layer," *Appl. Phys. Lett.*, vol. 91, p. 251902, Dec. 2007.

[36] F. Furtmayr, M. Vielemeyer, M. Stutzmann, J. Arbiol, S. Estrade, F. Peiro, J. R. Morante, and M. Eickhoff, "Nucleation and growth of GaN nanorods on Si (1 1 1) surfaces by plasma-assisted molecular beam epitaxy: The influence of Si- and Mg-doping," *J. Appl. Phys.*, vol. 104, p. 034309, Aug. 2008.

[37] C. T. Foxon, S. V. Novikov, J. L. Hall, R. P. Campion, D. Cherns, I. Griffiths, and S. Khongphetsak, "A complementary geometric model for the growth of GaN nanocolumns prepared by plasma-assisted molecular beam epitaxy," *J. Cryst. Growth*, vol. 311, pp. 3423–3427, 2009.

[38] Z. Liliental-Weber, "Defects in bulk GaN and homoepitaxial layers," in *Semiconductors and Semimetals: GaN Nitride (GaN) II*, vol. 57, J. I. Pankove and T. D. Moustakas, Eds. San Diego, CA: Academic, 1999, p. 132.

[39] L. Largeau, D. L. Dheeraj, M. Tchernycheva, G. E. Cirlin, and J. C. Harmand, "Facet and in-plane crystallographic orientations of GaN nanowires grown on Si(1 1 1)," *Nanotechnology*, vol. 19, p. 155704, Apr. 2008.

[40] K. A. Bertness, A. Roshko, L. M. Mansfield, T. E. Harvey, and N. A. Sanford, "Nucleation conditions for catalyst-free GaN nanowires," *J. Cryst. Growth*, vol. 300, pp. 94–99, 2007.

[41] H. Sekiguchi, T. Nakazato, A. Kikuchi, and K. Kishino, "Structural and optical properties of GaN nanocolumns grown on (0 0 0 1) sapphire substrates by rf-plasma-assisted molecular-beam epitaxy," *J. Cryst. Growth*, vol. 300, pp. 259–262, 2007.

[42] K. A. Bertness, A. Roshko, L. M. Mansfield, T. E. Harvey, and N. A. Sanford, "Mechanism for spontaneous growth of GaN nanowires with molecular beam epitaxy," *J. Cryst. Growth*, vol. 310, pp. 3154–3158, 2008.

[43] L. Cerutti, J. Ristić, S. Fernandez-Garrido, E. Calleja, A. Trampert, K. H. Ploog, S. Lazic, and J. M. Calleja, "Wurtzite GaN nanocolumns grown on Si(0 0 1) by molecular beam epitaxy," *Appl. Phys. Lett.*, vol. 88, p. 213114, May 2006.

[44] P. Corfdir, P. Lefebvre, J. Ristic, P. Valvin, E. Calleja, A. Trampert, J. D. Ganiere, and B. Deveaud-Pledran, "Time-resolved spectroscopy on GaN nanocolumns grown by plasma assisted molecular beam epitaxy on Si substrates," *J. Appl. Phys.*, vol. 105, p. 013113, Jan. 2009.

[45] E. Iliopoulosa, A. Adikimenakisa, E. Dimakisa, K. Tsagarakia, G. Konstantinidisa, and A. Georgakilas, "Active nitrogen species dependence on radiofrequency plasma source operating parameters and their role in GaN growth," *J. Cryst. Growth*, vol. 278, pp. 426–430, 2005.

[46] S. Fernández-Garrido, J. Grandal, E. Calleja, M. A. Sánchez-García, and D. López-Romero, "A growth diagram for plasma-assisted molecular beam epitaxy of GaN nanocolumns on Si(1 1 1)," *J. Appl. Phys.*, vol. 106, p. 126102, 2009.

[47] R. Calarco, R. J. Meijers, R. K. Debnath, T. Stoica, E. Sutter, and H. Luth, "Nucleation and growth of GaN nanowires on Si(1 1 1) performed by molecular beam epitaxy," *Nano Lett.*, vol. 7, pp. 2248–2251, Aug. 2007.

[48] J. Ristić, E. Calleja, S. Fernandez-Garrido, L. Cerutti, A. Trampert, U. Jahn, and K. H. Ploog, "On the mechanisms of spontaneous growth of III-nitride nanocolumns by plasma-assisted molecular beam epitaxy," *J. Cryst. Growth*, vol. 310, pp. 4035–4045, Aug. 2008.

[49] R. Meijers, T. Richter, R. Calarco, T. Stoica, H. P. Bochem, M. Marso, and H. Luth, "GaN-nanowhiskers: MBE-growth conditions and optical properties," *J. Cryst. Growth*, vol. 289, pp. 381–386, Mar. 2006.

[50] B. Heying, R. Averbeck, L. F. Chen, E. Haus, H. Riechert, and J. S. Speck, "Control of GaN surface morphologies using plasma-assisted molecular beam epitaxy," *J. Appl. Phys.*, vol. 88, pp. 1855–1860, 2000.

[51] K. A. Bertness, "Smart pyrometry for combined sample temperature and reflectance measurements in molecular beam epitaxy," *J. Vac. Sci. Technol. B*, vol. 18, pp. 1426–1430, 2000.

[52] E. Calleja, M. A. Sánchez-García, F. J. Sánchez, F. Calle, F. B. Naranjo, E. Muñoz, U. Jahn, and K. Ploog, "Luminescence properties and defects in GaN nanocolumns grown by molecular beam epitaxy," *Phys. Rev. B*, vol. 62, pp. 16826–16834, 2000.

[53] K. A. Bertness, N. A. Sanford, J. M. Barker, J. B. Schlager, A. Roshko, A. V. Davydov, and I. Levin, "Catalyst-free growth of GaN nanowires," *J. Electron. Mat.*, vol. 35, pp. 576–580, 2006.

[54] K. A. Bertness, A. Roshko, N. A. Sanford, J. M. Barker, and A. V. Davydov, "Spontaneously grown GaN and AlGaN nanowires," *J. Cryst. Growth*, vol. 287, pp. 522–527, 2006.

[55] L. Lymperakis and J. Neugebauer, "Large anisotropic adatom kinetics on nonpolar GaN surfaces: Consequences for surface morphologies and nanowire growth," *Phys. Rev. B*, vol. 79, p. 241308, Jun. 2009.

[56] R. K. Debnath, R. Meijers, T. Richter, T. Stoica, R. Calarco, and H. Luth, "Mechanism of molecular beam epitaxy growth of GaN nanowires on Si(1 1 1)," *Appl. Phys. Lett.*, vol. 90, p. 123117, Mar. 2007.

[57] T. Stoica, E. Sutter, R. J. Meijers, R. K. Debnath, R. Calarco, H. Luth, and D. Grutzmacher, "Interface and wetting layer effect on the catalyst-free nucleation and growth of GaN nanowires," *Small*, vol. 4, pp. 751–754, Jun. 2008.

[58] C. T. Foxon, T. S. Cheng, N. J. Jeffs, J. Dewsnip, L. Flannery, J. W. Orton, I. Harrison, S. V. Novikov, B. Y. Ber, and Y. A. Kudriavtsev, "Studies of

p-GaN grown by MBE on GaAs(1 1 1)B," *J. Cryst. Growth*, vol. 190, pp. 516–518, Jun. 1998.
[59] V. Consonni, M. Knelangen, L. Geelhaar, A. Trampert, and H. Riechert, "Nucleation mechanisms of epitaxial GaN nanowires: Origin of their self-induced formation and initial radius," *Phys. Rev. B*, vol. 81, p. 085310, Feb. 2010.
[60] S. D. Hersee, X. Y. Sun, and X. Wang, "The controlled growth of GaN nanowires," *Nano Lett.*, vol. 6, pp. 1808–1811, 2006.
[61] P. Deb, H. Kim, V. Rawat, M. Oliver, S. Kim, M. Marshall, E. Stach, and T. Sands, "Faceted and Vertically Aligned GaN Nanorod Arrays Fabricated without Catalysts or Lithography," *Nano Lett.*, vol. 5, pp. 1847–1851, 2005.
[62] S. Ishizawa, H. Sekiguchi, A. Kikuchi, and K. Kishino, "Selective growth of GaN nanocolumns by Al thin layer on substrate," *Physica. Status Solidi B-Basic Solid State Physics*, vol. 244, pp. 1815–1819, Jun. 2007.
[63] K. A. Bertness, A. W. Sanders, D. M. Rourke, T. E. Harvey, A. Roshko, J. B. Schlager, and N. A. Sanford, "Controlled Nucleation of GaN Nanowires Grown with Molecular Beam Epitaxy," *Adv. Functional Mater.*, vol. 20, no. 17, pp. 2911–2951, Sep. 2010.
[64] A. Trampert, J. Ristic, U. Jahn, E. Calleja, and K. H. Ploog, "TEM study of (Ga,Al)N nanocolumns and embedded GaN nanodiscs," in *Microscopy of Semiconducting Materials 2003*. vol. 180, Bristol, PA: IOP, 2003, pp. 167–170.
[65] V. Consonni, M. Knelangen, U. Jahn, A. Trampert, L. Geelhaar, and H. Riechert, "Effects of nanowire coalescence on their structural and optical properties on a local scale," *Appl. Phys. Lett.*, vol. 95, p. 241910, Dec. 2009.
[66] L. H. Robins, K. A. Bertness, J. M. Barker, N. A. Sanford, and J. B. Schlager, "Optical and structural study of GaN nanowires grown by catalyst-free molecular beam epitaxy. II. Subbandgap luminescence and electron irradiation effects," *J. Appl. Phys.*, vol. 101, p. 113506, Jun. 2007.
[67] D. Cherns, L. Meshi, I. Griffiths, S. Khongphetsak, S. V. Novikov, N. R. S. Farley, R. P. Campion, and C. T. Foxon, "Defect-controlled growth of GaN nanorods on (0 0 0 1) sapphire by molecular beam epitaxy," *Appl. Phys. Lett.*, vol. 93, p. 111911, Sep. 2008.
[68] J. D. Eshelby, "Screw dislocations in thin rods," *J. Appl. Phys.*, vol. 24, pp. 176–179, 1953.
[69] D. Tham, C.-Y. Nam, and J. E. Fischer, "Defects in GaN Nanowires," *Adv. Functional Mater.*, vol. 16, pp. 1197–1202, 2006.
[70] L. Dai, S. F. Liu, L. P. You, J. C. Zhang, and G. G. Qin, "Effects of In surfactant on the crystalline and photoluminescence properties of GaN nanowires," *J. Phys.:Condens. Matter*, vol. 17, pp. L445–L449, 2005.
[71] B. Ha, S. H. Seo, J. H. Cho, C. S. Yoon, J. Yoo, G.-C. Yi, C. Y. Park, and C. J. Lee, "Optical and field emission properties of thin single-crystalline GaN nanowires," *J. Phys. Chem. B*, vol. 109, pp. 11095–11099, 2005.
[72] C. Cheze, L. Geelhaar, O. Brandt, H. Riechert, S. Muench, R. Rothemund, S. Reitzenstein, A. Forchel, T. Kehagias, P. Komninou, G. P. Dimitrakopulos, and T. Karakostas, "Direct comparison of catalyst-induced and catalyst-free GaN nanowires," in *Proc. Mater. Res. Soc. (MRS) Fall Symp.*, Boston, MA, 2009, p. M12.6.
[73] A. A. Talin, G. T. Wang, E. Lai, and R. J. Anderson, "Correlation of growth temperature, photoluminescence, and resistivity in GaN nanowires," *Appl. Phys. Lett.*, vol. 92, p. 093105, Feb. 2008.
[74] J. Grandal, M. A. Sanchez-Garcia, E. Calleja, E. Gallardo, J. M. Calleja, E. Luna, A. Trampert, and U. Jahn, "InN nanocolumns grown by plasma-assisted molecular beam epitaxy on A-plane GaN templates (vol 94, p. 221908, 2009)," *Appl. Phys. Lett.*, vol. 95, p. 221908, Jul. 2009.
[75] C. H. Shen, H. Y. Chen, H. W. Lin, S. Gwo, A. A. Klochikhin, and V. Y. Davydov, "Near-infrared photoluminescence from vertical InN nanorod arrays grown on silicon: Effects of surface electron accumulation layer," *Appl. Phys. Lett.*, vol. 88, p. 253104, Jun. 2006.
[76] T. Stoica, R. Meijers, R. Calarco, T. Richter, and H. Luth, "MBE growth optimization of InN nanowires," *J. Cryst. Growth*, vol. 290, pp. 241–247, Apr. 2006.
[77] O. Landre, V. Fellmann, P. Jaffrennou, C. Bougerol, H. Renevier, A. Cros, and B. Daudin, "Molecular beam epitaxy growth and optical properties of AlN nanowires," *Appl. Phys. Lett.*, vol. 96, p. 061912, Feb. 2010.
[78] R. Armitage and K. Tsubaki, "Multicolour luminescence from InGaN quantum wells grown over GaN nanowire arrays by molecular-beam epitaxy," *Nanotechnology*, vol. 21, p. 195202, May 2010.
[79] J. Ristić, E. Calleja, A. Trampert, S. Fernandez-Garrido, C. Rivera, U. Jahn, and K. H. Ploog, "Columnar AlGaN/GaN nanocavities with AlN/GaN Bragg reflectors grown by molecular beam epitaxy on Si(1 1 1)," *Phys. Rev. Lett.*, vol. 94, Apr. 2005.
[80] J. Ristić, E. Calleja, M. A. Sánchez-García, J. M. Ulloa, J. Sánchez-Paramo, J. M. Calleja, U. Jahn, A. Trampert, and K. H. Ploog, "Characterization of GaN quantum discs embedded in AlxGa1-xN nanocolumns grown by molecular beam epitaxy," *Phys. Rev. B*, vol. 68, pp. 125305-1–125305-5, 2003.
[81] C. Rivera, U. Jahn, T. Flissikowski, J. L. Pau, E. Muñoz, and H. T. Grahn, "Strain-confinement mechanism in mesoscopic quantum disks based on piezoelectric materials," *Phys. Rev. B*, vol. 75, p. 045316, 2007.
[82] A. Kikuchi, M. Tada, K. Miwa, and K. Kishino, "Growth and characterization of InGaN/GaN nanocolumn LED," in *Proc. SPIE Quantum Dots, Particles and Nanoclusters III*, 2006, p. 612905-1.
[83] J. B. Schlager, N. A. Sanford, K. A. Bertness, J. M. Barker, A. Roshko, and P. T. Blanchard, "Polarization-resolved photoluminescence study of individual GaN nanowires grown by catalyst-free MBE," *Appl. Phys. Lett.*, vol. 88, p. 213106, 2006.
[84] N. Thillosen, K. Sebald, H. Hardtdegen, R. Meijers, R. Calarco, S. Montanari, N. Kaluza, J. Gutowski, and H. Lüth, "The State of Strain in Single GaN Nanocolumns As Derived from MicroPhotoluminescence Measurements," *Nano Lett.*, vol. 6, pp. 704–708, 2006.
[85] M. Tchernycheva, C. Sartel, G. Cirlin, L. Travers, G. Patriarche, J. C. Harmand, L. S. Dang, J. Renard, B. Gayral, L. Nevou, and F. Julien, "Growth of GaN free-standing nanowires by plasma-assisted molecular beam epitaxy: structural and optical characterization," *Nanotechnology*, vol. 18, p. 385306, Sep. 2007.
[86] I. Levin, NIST, Gaithersburg, MD, unpublished data, Jun. 2010.
[87] A. W. Sanders, NIST, Boulder, CO, private communication, Jun. 2010.
[88] J. B. Schlager, K. A. Bertness, P. T. Blanchard, L. H. Robins, A. Roshko, and N. A. Sanford, "Steady-state and time-resolved photoluminescence from relaxed and strained GaN nanowires grown by catalyst-free molecular-beam epitaxy," *J. Appl. Phys.*, vol. 103, p. 124309, Jun. 2008.
[89] O. Brandt, C. Pfuller, C. Cheze, L. Geelhaar, and H. Riechert, "SubmeV linewidth of excitonic luminescence in single GaN nanowires: Direct evidence for surface excitons," *Phys. Rev. B*, vol. 81, p. 045302, Jan. 2010.
[90] M. A. Reshchikov and H. Morkoç, "Luminescence properties of defects in GaN," *J. Appl. Phys.*, vol. 97, p. 061301, 2005.
[91] J. Lloyd-Hughes, S. K. E. Merchant, L. Fu, H. H. Tan, C. Jagadish, E. Castro-Camus, and M. B. Johnston, "Influence of surface passivation on ultrafast carrier dynamics and terahertz radiation generation in GaAs," *Appl. Phys. Lett.*, vol. 89, p. 232102, Dec. 2006.
[92] S. Watanabe, N. Yamada, M. Nagashima, Y. Ueki, C. Sasaki, Y. Yamada, T. Taguchi, K. Tadatomo, H. Okagawa, and H. Kudo, "Internal quantum efficiency of highly-efficient InxGa1-xN-based near-ultraviolet light-emitting diodes," *Appl. Phys. Lett.*, vol. 83, pp. 4906–4908, Dec. 2003.
[93] J. B. Schlager, N. A. Sanford, K. A. Bertness, and A. Roshko, "Injection-level-dependent internal quantum efficiency and lasing in low-defect GaN nanowires," submitted for publication, 2010.
[94] L. H. Robins, K. A. Bertness, J. M. Barker, N. A. Sanford, and J. B. Schlager, "Optical and structural study of GaN nanowires grown by catalyst-free molecular beam epitaxy. I. Near-band-edge luminescence and strain effects," *J. Appl. Phys.*, vol. 101, p. 113505, Jun. 2007.
[95] L. Baird, G. H. Ang, C. H. Low, N. M. Haegel, A. A. Talin, Q. Li, and G. T. Wang, "Imaging minority carrier diffusion in GaN nanowires using near field optical microscopy," *Physica B: Condensed Matter*, vol. 404, pp. 4933–4936, 2009.
[96] Y. Huang, X. Duan, Y. Cui, and C. M. Lieber, "GaN nanowire devices," *Nano Lett.*, vol. 2, p. 101, 2002.
[97] H.-Y. Cha, H. Wu, M. Chandrashekhar, Y. C. Choi, S. Chae, G. Koley, and M. G. Spencer, "Fabrication and characterization of prealigned gallium nitride nanowire field-effect transistors," *Nanotechnology*, vol. 17, pp. 1264–1271, 2006.
[98] O. Wunnicke, "Gate capacitance of back-gated nanowire field-effect transistors," *Appl. Phys. Lett.*, vol. 89, p. 083102, Aug. 2006.
[99] D. R. Khanal and J. Wu, "Gate coupling and charge distribution in nanowire field effect transistors," *Nano Lett.*, vol. 7, pp. 2778–2783, Sep. 2007.
[100] L. M. Mansfield, K. A. Bertness, P. T. Blanchard, T. E. Harvey, A. W. Sanders, and N. A. Sanford, "GaN nanowire carrier concentration calculated from light and dark resistance measurements," *J. Electron. Mat.*, vol. 38, pp. 495–504, 2009.
[101] N. A. Sanford, P. T. Blanchard, K. A. Bertness, L. Mansfield, J. B. Schlager, A. W. Sanders, A. Roshko, B. B. Burton, and S. M. George, "Steady-state and transient photoconductivity in *c*-axis GaN nanowires

grown by nitrogen-plasma-assisted molecular beam epitaxy," *J. Appl. Phys.*, vol. 107, p. 034318, Feb 2010.

[102] S. Nikishin, G. Kipshidze, V. Kuryatkov, K. Choi, Ì. Gherasoiu, L. Grave de Peralta, A. Zubrilov, V. Tretyakov, K. Copeland, T. Prokofyeva, M. M. Holtz, R. Asomoza, Y. Kudryavtsev, and H. Temkin, "Gas source molecular beam epitaxy of high quality AlxGa1–*x*N ($0 \leq x \leq 1$) on Si(1 1 1)," *J. Vac. Sci. Technol. B*, vol. 19, pp. 1409–1412, 2001.

[103] M. Kočan, A. Rizzi, H. Lüth, S. Keller, and U. K. Mishra, "Surface potential at as-grown GaN(0 0 0 1) MBE Layers," *Phys. Stat. Sol. (b)*, vol. 234, pp. 773–777, 2002.

[104] M. A. Reshchikov, S. Sabuktagin, D. K. Johnstone, and H. Morkoç, "Transient photovoltage in GaN as measured by atomic force microscope tip," *J. Appl. Phys.*, vol. 96, pp. 2556–2560, Sep. 2004.

[105] M. A. Reshchikov, M. Foussekis, and A. A. Baski, "Surface photovoltage in undoped n-type GaN," *J. Appl. Phys.*, vol. 107, p. 113535, Sep. 2010.

[106] S. Chevtchenko, X. Ni, Q. Fan, A. A. Bask, and H. Morkoç, "Surface band bending of a-plane GaN studied by scanning Kelvin probe microscopy," *Appl. Phys. Lett.*, vol. 88, p. 122104, 2006.

[107] S. Tiwari, *Compound Semiconductor Device Physics*. San Diego, CA: Academic, 1992.

[108] A. Many, Y. Goldstein, and N. B. Grover, *Semiconductor Surfaces*. Amsterdam, The Netherlands: North-Holland, 1965.

[109] A. Armstrong, G. T. Wang, and A. A. Talin, "Depletion-mode photoconductivity study of deep levels in GaN nanowires," *J. Electron. Mat.*, vol. 38, pp. 484–489, 2009.

[110] C.-J. Chiang, T. M. Wallis, D. Gu, A. Imtiaz, P. Kabos, P. T. Blanchard, K. A. Bertness, N. A. Sanford, K. Kim, and D. Filipovic, "High frequency characterization of a Schottky contact to a GaN nanowire bundle," *J. Appl. Phys.*, vol. 107, p. 124301, 2010.

[111] S. M. Tanner, J. M. Gray, C. T. Rogers, K. A. Bertness, and N. A. Sanford, "High-Q GaN nanowire resonators and oscillators," *Appl. Phys. Lett.*, vol. 91, p. 203117, Nov. 2007.

[112] C.-Y. Nam, P. Jaroenapibal, D. Tham, D. E. Luzzi, S. Evoy, and J. E. Fischer, "Diameter-dependent electromechanical properties of GaN nanowires," *Nano Lett.*, vol. 6, pp. 153–158, 2006.

[113] J. R. Montague, M. Dalberth, J. M. Gray, D. Seghete, K. A. Bertness, S. M. George, V. M. Bright, and N. A. Sanford, "High-Q, gallium nitride nanowire resonators for thin-film deposition sensor applications," *Sensors Actuat. A: Physical*, to be published. DOI: 10.1016/j.sna.2010.03.014.

[114] J. J. Brown, A. I. Baca, K. A. Bertness, D. A. Dikin, R. S. Ruoff, and V. M. Bright, "Tensile measurement of single crystal gallium nitride nanowires on MEMS test stages," *Sensors and Actuators A: Physical*, to be published. DOI: 10.1016/j.sna.2010.04.002.

[115] J. R. Montague, University of Colorado, Boulder, private communication, Jun. 2010.

[116] J. M. Gray, University of Colorado, Boulder, private communication, Jun. 2010.

Kris A. Bertness (M'00–SM'01) received the B.A. degree from Oberlin College, Oberlin, OH, in 1981, and the Ph.D. degree in physics from Stanford University, Stanford, CA, in 1987.

She is currently an Acting Group Leader in the Optoelectronics Division, National Institute of Standards and Technology (NIST), Boulder, CO. Prior to joining NIST in 1995, she developed record-efficiency solar cells at the National Renewable Energy Laboratory and at Varian Research Center. Her technical research interests include III–V semiconductor crystal growth, characterization, and device design, including research on nanowires and quantum dots.

Norman A. Sanford received the B.S. degree in physics from Western Washington State College, Bellingham, in 1976, and the Ph.D. degree in physics from Rensselaer Polytechnic Institute, Rensselaer, NY, 1983.

He is currently a Project Leader of the Semiconductor Metrology for Energy Conversion Project of the National Institute of Standards and Technology (NIST), Boulder, CO. His research interests include rare-earth-doped waveguide lasers, nonlinear optical characterization of materials, X-ray studies of wide-band-gap III-nitrides, and most recently, characterization of wide-bandgap III-nitride nanowires.

Dr. Sanford is a Fellow of the Optical Society of America.

Albert V. Davydov received the Ph.D.degree in chemistry from Moscow State University, Moscow, Russia, in 1989.

Since 1997, he has been with National Institute of Standards and Technology (NIST), Gaithersburg, MD, which received the R&D Micro/Nano 25 award in 2006 for his and other author's work on GaN nanowires. He is currently the Head of the Semiconductor Task Group for the International Centre for Diffraction Data at NIST. His research interests include processing and characterization of electronic materials, i.e., nanowire, thin film, and bulk crystal growth, structural characterization of nanowires, films and bulk crystals, metallization of GaN, and experimental and computational study of phase diagrams.